

The analysis of dynamic effects in the frog part of railway switches

SMUTNY Jaroslav^{1,a}, JANOSTIK Dusan^{1,b}, NOHAL Viktor^{1,c} and
PAZDERA Lubos^{2,a}

¹Institute of Railway Structures and Constructions, Faculty of Civil Engineering; Brno
University of Technology; Veveri 331/95, 602 69 Brno, Czech Republic

²Institute of Physics, Faculty of Civil Engineering; Brno University of Technology;
Zizkova 331/17, 602 69 Brno, Czech Republic

^asmutny.j@fce.vutbr.cz, ^bjanostik.d@fce.vutbr.cz, ^cnohal.v@fce.vutbr.cz,
^dpazdera.l@fce.vutbr.cz

Keywords: Railway switch, dynamic effects, vibration analysis in time and frequency domain, non-linear time-frequency transformation, Zhao-Atlas-Marks transformation

Abstract. This paper deals with description and application of the Zhao-Atlas-Marks transformation for dynamic analysis. This transformation belongs to the group of non-linear time-frequency processes. Thanks to its properties it may be successfully used in the area of non-stationary and transitional signals describing various natural processes. The use in the field of railway constructions testing represents a quite interesting application area of the transformation. This paper contains a mathematical description of the transformation; a case study from the area of railway switches dynamic analysis and practical experience obtained and recommendations for its practical use.

Introduction

The fundamental requirements of the particular parts of the railway track are their functional reliability and the safety of the interconnected railway operation. Although the superstructure has been developed nearly to the perfection during more than 150 years of the railway history, it is still possible to find new technical solutions. This especially applies to various types of switches structures, various rail fastenings, various types of rail pads, sleepers etc.

Permanent pressure to increase the transport speed and the operational load on the railway resulted in huge development of new technologies. The decision on modernization of the corridors became the impulse for development of all areas of the railway transport, both in the area of vehicles and infrastructure. In correspondence with the above-mentioned trend, the application of new experimental processes should continue to evaluate the quality and suitability of individual constructional solutions.

The level of dynamic effects in the railway superstructure is influenced by its quality, operational and technical conditions, climatic events and, most importantly by dynamic load on the railway vehicle axle. The fact also relates to construction of the railway switches representing the key points of the railway roads.

The railway switch structures represent one of the key points of the railway transport. Therefore it is necessary to pay a special attention to these structures. The switch structure consists of a number of structural components of different properties which in summary must fulfil the required functions. The most important properties are particularly their reliability and safety within the framework of the railway operation [1].

In accordance to this trend, the development and application of new experimental

procedures for assessing the quality and effectiveness of individual design solutions must also proceed.

Zhao-Atlas-Marks transformation

Information about any technical event is represented in the signal by time changes of the instantaneous value of the physical quantity described by the signal. There are a number of methods in the time plane that can be applied to the measured signal. These include the search for global and local highs and lows depending on time, correlation analysis, analysis of signal attenuation, or different statistical methods, etc.

In some cases, important information about the analysed frequency domain event can be obtained. The Fourier transform is the most widely used and best known method to convert from time to frequency domain. Often, it is necessary to analyse non-stationary processes, i.e. events where the frequency content of the signal varies with time.

One of the possible ways to analyse the time incidence of frequency components, especially in transient and non-stationary signals, is to use the so-called time-frequency transformations. These can be divided into two basic classes according to the computational process [2]:

- linear (these include, in particular, Short-Term Fourier Transform and Wavelet Transform)
- nonlinear (include, in particular, quadratic Cohen, affine, and hyperbolic transformations, and other special techniques)

Zhao-Atlas-Marks transform belongs to the class of so-called quadratic, time and frequency invariant transformations. The biggest advantage of this group of transformations is the fact that their resulting resolution in time and frequency is not limited by the so-called Heisenberg uncertainty principle. This is manifested by the high resolution of the transformations in the time-frequency plane. At the same time the so-called core function determines the properties of a particular transformation. It is generally assumed that any quadratic, temporal, and frequency-invariant transformations can be expressed by [3]

$$CT_x(t, \omega) = \int_{-\infty}^{\infty} \int_{-\infty}^{\infty} \Pi(\tau - t, \theta - \omega) \cdot WVT(\tau, \theta) \cdot d\tau \cdot d\theta, \quad (1)$$

where

$$\Pi(t, \omega) = \int_{-\infty}^{\infty} \int_{-\infty}^{\infty} \psi(\theta, \tau) \cdot e^{-j \cdot 2 \cdot \pi \cdot (\omega \cdot \tau - \theta \cdot t)} \cdot dt \cdot d\omega. \quad (2)$$

Note that WVT represents the coefficients of the Wigner-Vill transform, Π is the two-dimensional Fourier transform of the core function ψ , the symbol τ represents the time shift, t is the time, ω is the angular frequency, θ the frequency shift and j is complex operator.

The core function for Zhao-Atlas-Marks transformation is defined by [4]

$$\psi(\theta, \tau) = h(\tau) \cdot \frac{\sin a \cdot \theta \cdot \tau}{a \cdot \theta \cdot \tau}, \quad (3)$$

where $h(\tau)$ represents a window function, a is a suitably selected parameter for suppressing interference components. In practice, the coefficients of the individual quadratic, temporally and frequency-invariant CT_x transformations for discrete signals can be calculated by the fast two-dimensional Fourier transform of the discrete characteristic function $A_x(n, k) \cdot \psi(n, k)$. $A_x(n, k)$ is defined by the equation (4)

$$A_x(\theta, \tau) = \int_{-\infty}^{\infty} x\left(t + \frac{\tau}{2}\right) \cdot x^*\left(t - \frac{\tau}{2}\right) \cdot e^{j\theta t} \cdot dt. \quad (4)$$

It is a "narrow-band" function that is complex and represents a measure of the time-frequency correlation of a signal, or expresses the degree of similarity between a signal and its shifted version in a time-frequency plane. Thus, it is essentially a time-frequency autocorrelation function.

Case study

The following text presents the use of Zhao-Atlas-Marks transformation in the field of railway engineering. It was an analysis of dynamic effects in the frog part of two switches. Let us note that the frog section formed by wing rails, the frog wedge and the frog rails connected to the frog wedge belong to the most stressed places of the railway line.

The monitored switches no. 3 and no. 4 (Fig. 1) are situated in Třebová station head of the railway station in Ústí nad Orlicí. Both switches are located on a high embankment. They have the same slenderness (1:12 - 500), both are mostly driven by the frog tip and have the same frogs (UIC 60 shape, ZPT frog type - monoblock). Switch no. 4 has a classic fastening with ribbed bases on concrete sleepers with Skl 24 clamps and is located in track no. 2. Switch no. 3 has a new type of rail fastening UNO3718 with ribbed bases on concrete sleepers with Skl 24 clamps and is located in rail no. 1. The main difference between the aforementioned fasteners is primarily in the base under the rail foot. The measurements were performed in March 2019.



Fig. 1: View of rail coupling with switches 3 and 4.

Vibration measurement and analysis methodology was used to test both switches designs. The next part of the paper is devoted to the analysis of vibration transmission passing from the frog through the sleeper to the rail bed. Vibration characteristics were obtained based on the response of tested structures to moving loads, i.e. trainsets. Vibration-accelerating piezoelectric transducers were used to measure the dynamic-effect characteristics. Within this methodology, the sensors are positioned to be able to capture the spreading of vibration energy throughout the system. A three-axis accelerometer located on the foot of the wing rail monitors the magnitude of the dynamic impact that acts on the frog of the switch. In the vertical direction (A_{WRZ}), the size of the vertical component of the dynamic impact is captured on the frog, respectively the part to be transferred to the foot of the wing rail. Depending on

the state of the crossing geometry, a larger or smaller part of the dynamic impact is also realized in the longitudinal direction (A_{WRZ}). In the transverse direction (A_{WRY}), the wheelset is guided by a retainer. The lateral impact on the frog is very small, but it is interesting to observe this component only from the point of view of the smoothness of the train passing through the switch, therefore, this component is also monitored within the proposed methodology. The other sensors were uniaxial and were positioned to best capture the dynamic impact spreading from the frog crossing through the sleeper to the ballast bed. The A_{SZ} sensor was placed on the sleeper under the frog tip and the A_{BBZ} sensor on the so-called measuring rod (waveguide), which was embedded in the ballast bed near the frog tip.

Note that dynamic parameter measurement was performed after the frog replacement. At both switches, a frog with a high-manganese cast steel central section reinforced by an explosion was installed.

Let us first consider comparing the maximum and minimum vibration acceleration values at the transition from the wing rail to the ballast bed in the time domain.

Tab. 1: The comparison of the maximum values of vibration acceleration

Construction	Train	V [km/h]	a [m/s ²]					
			A_{WRZ}		A_{SZ}		A_{BBZ}	
			Min	Max	Min	Max	Min	Max
3	RailJet	130	-559	719	-80	70	-28	29
4	RailJet	130	-507	515	-141	150	-65	60
3	Pendolino	150	-712	997	-68	65	-79	31
4	Pendolino	150	-477	510	-117	134	-62	60
3	Leo Express	130	-638	839	-70	62	-40	33
4	Leo Express	130	-453	379	-132	145	-59	53
3	RegioJet	130	-729	776	-98	86	-38	43
4	RegioJet	130	-564	497	-132	185	-70	65
3	R 380	130	-696	816	-100	110	-57	32
4	R 380	130	-462	496	-115	157	-73	51

Tab. 2: The comparison of effective vibration acceleration values

Construction	Train	V [km/h]	aef [m/s ²]		
			A_{WRZ}	A_{SZ}	A_{BBZ}
3	RailJet	130	65	10	4
4	RailJet	130	52	18	7
3	Pendolino	150	80	11	3
4	Pendolino	150	70	16	6
3	Leo Express	130	65	9	3
4	Leo Express	130	50	17	6
3	RegioJet	130	67	12	4
4	RegioJet	130	59	20	8
3	380	130	67	11	3
4	380	130	43	14	5

Comparing values indicated in the table Tab. 1 shows that on the wing rail in the vertical direction (A_{WRZ}) higher values were found at the switch no. 3. Values on the sleeper at the crossing frog (A_{SZ}) and at the ballast bed (A_{BBZ}) are already higher at switch no. 4, and the difference is quite significant. Significantly higher vibration acceleration values at the frog sleeper (A_{SZ}) and in the ballast bed (A_{BBZ}) at switch no. 4, mean that more peak values are transmitted to the sleeper and ballast bed. Similar results are shown in Table 2. Note that this table shows comparison of effective acceleration values.

Because of the limited number of pages, the next measurement outputs are presented only for the position of the accelerometer on the sleeper under the frog. The analysis outputs were implemented into three graphs. The upper graph of each image shows the time course of the vibration acceleration. The amplitude spectrum of the vibration response is displayed in the left graph. The middle graph shows a 3D representation of the time-frequency course of the amplitude spectrum of the vibration response. Spectral values are expressed in decibel scale by different colors (or grayscale). Note that the maximum value is black.

It can be seen from the comparison of the amplitude spectra (Fig. 3, Fig. 4) that the calculated spectra are different for both structures. On the wing rail of switch no. 3, the maximum spectrum values at higher frequencies were reached than at switch no. 4. It is already apparent on the sleeper that the shape of the spectra is similar for both structures. The maximum spectral values were reached at switch no. 4.

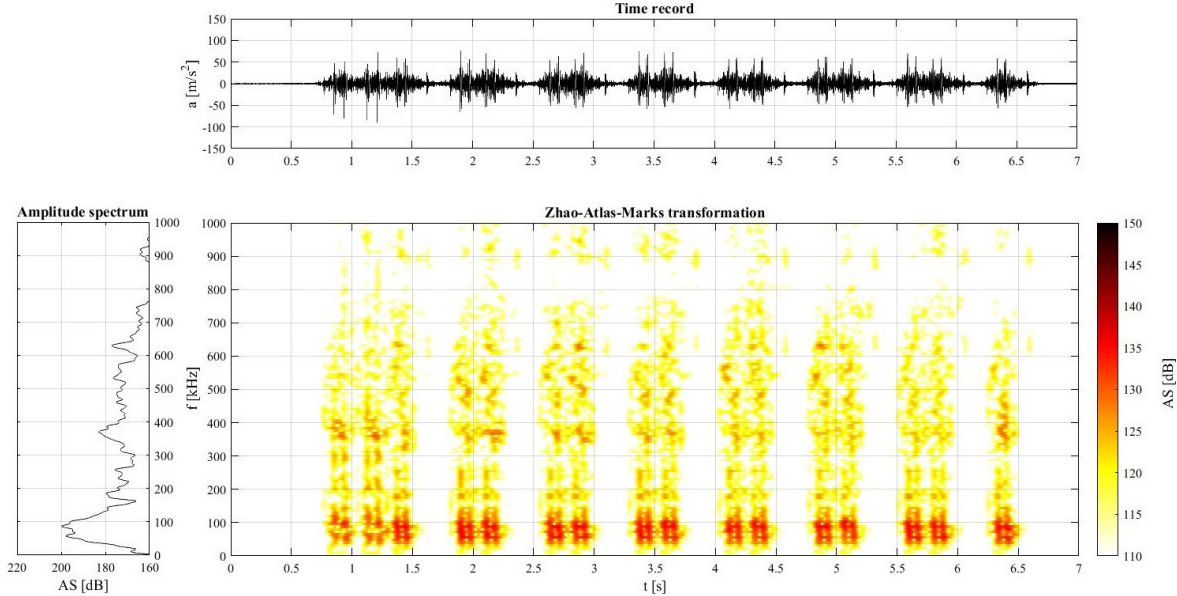


Fig. 2: Time, frequency and time-frequency characteristics of the vibrations, sensor on the sleeper, switch no. 3, vertically direction, RailJet, speed 130 km·h⁻¹

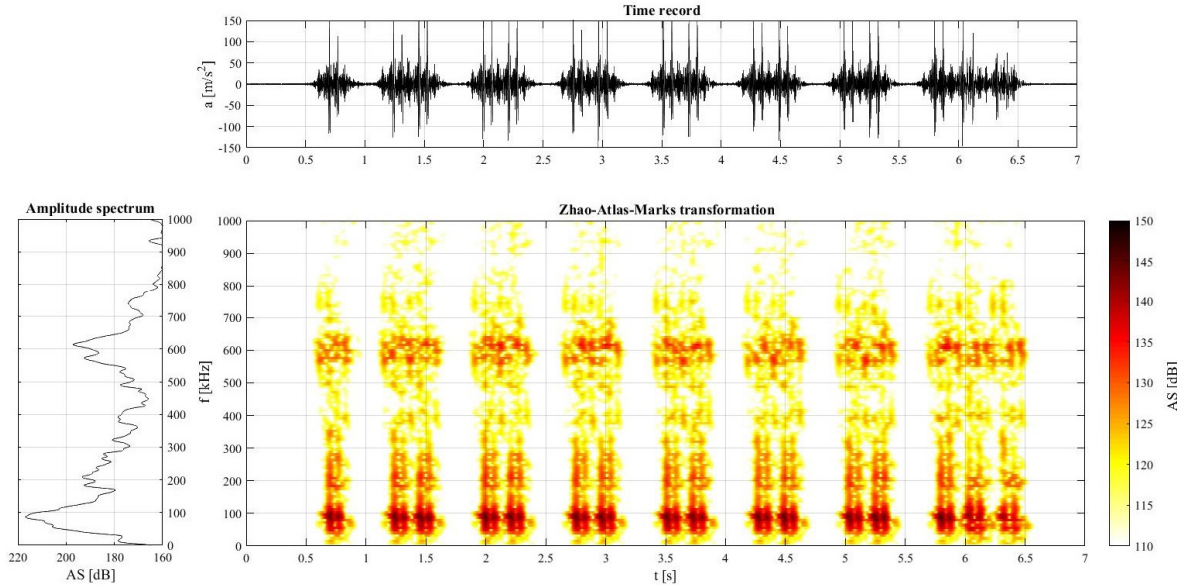


Fig. 3: Time, frequency and time-frequency characteristics of the vibrations, sensor on the sleeper, switch no. 4, vertically direction, RailJet, speed 130 km·h⁻¹

The same conclusions are confirmed by the time-frequency analysis of the Zhao-Atlas-Marks transformation. As can be seen from the middle graphs (Figs. 3 and 4) compared to time and frequency analysis, there is a time localization of significant frequency components.

It is therefore possible to deduce a positive influence of the elasticity in the fastening node from the presented graphs. The new rail fastening node UNO3718 on switch no. 3, even after frog replacement, better dampens peak vibration acceleration values compared to conventional fastening at switch no. 4. In this way the ballast bed is better protected from gradual degradation.

Conclusions

Zhao-Atlas-Marks transformation offers a comprehensive tool for analysing non-stationary signals in particular. Characteristic feature of presented transformation is the fact that its resulting distinguishment in time and frequency is not limited by Heisenberg principle of indefiniteness. This fact includes the high distinguishing ability in the time frequency plane that gives rise to a “precise” localisation of important frequency components in time. This method gives a fast and accurate localisation of frequency components included in the measured signal.

From the vibration measurement analysis in both switches the positive influence of the elasticity in the fastening node can be evaluated. On the sleeper under the frog, there is a smaller vibration acceleration value at the switch no. 3 than at switch no. 4. Elasticized fastening node increases vertical elasticity of superstructure, which ultimately leads to a further reduction of wear and disintegration of aggregate of the ballast bed. In this way, the upper of the switch is protected and the quality of the crossover geometric parameters is maintained. This solution offers railway managers the opportunity to significantly reduce the annual maintenance costs of railway lines.

Acknowledgments

This paper has been worked out under the research project FAST-S-19-5797, The analysis of dynamic response of railway track construction by the affine time frequency transformations method.

References

- [1] Moravcik M.: Analysis of vehicle bogie effects on track structure-nonstationary analysis of dynamic response, Communications, Volume 13, 3/2011, EDIS Zilina, ISSN 1335-4205
- [2] Smutný, J.; Pazdera, L., The experimental analysis of dynamic processes related to railway transport, monography, ISBN 978-80-7204-827-4, AKADEMICKÉ NAKLADATELSTVÍ CERM, Brno, 2012
- [3] Smutný J.: Measurement and Analysis of Dynamic and Acoustic Parameters of Rail Fastening, NDT & E International - Independent Nondestructive Testing and Evaluation, 2004, Volume 37, Issues 8, ELSEVIER, pp. 119-129, ISSN 0963-8695
- [4] Smutný J., Pazdera L.: New Techniques in Analysis of Dynamic Parameters Rail Fastening, InSight, The Journal of The British Institute of Non-Destructive Testing. Vol 46. No 10. October. 2004. pp. 612-615. ISSN 13542575